HHS Public Access

Author manuscript

Neuroscience. Author manuscript; available in PMC 2019 January 01.

Published in final edited form as:

Neuroscience. 2018 January 01; 368: 57–69. doi:10.1016/j.neuroscience.2017.09.003.

Neocortical Dynamics during Whisker-based Sensory Discrimination in Head-Restrained Mice

Fritjof Helmchen, **Ariel Gilad**, and **Jerry L. Chen***

Laboratory of Neural Circuit Dynamics, Brain Research Institute, University of Zurich, Switzerland

Abstract

A fundamental task frequently encountered by brains is to rapidly and reliably discriminate between sensory stimuli of the same modality, be it distinct auditory sounds, odors, visual patterns, or tactile textures. A key mammalian brain structure involved in discrimination behavior is the neocortex. Sensory processing not only involves the respective primary sensory area, which is crucial for perceptual detection, but additionally relies on cortico-cortical communication among several regions including higher-order sensory areas as well as frontal cortical areas. It remains elusive how these regions exchange information to process neural representations of distinct stimuli to bring about a decision and initiate appropriate behavioral responses. Likewise, it is poorly understood how these neural computations are conjured during task learning. In this review, we discuss recent studies investigating cortical dynamics during discrimination behaviors that utilize head-fixed behavioral tasks in combination with in vivo electrophysiology, two-photon calcium imaging, and cell-type specific targeting. We particularly focus on information flow in distinct cortico-cortical pathways when mice use their whiskers to discriminate between different objects or different locations. Within the primary and secondary somatosensory cortices (S1 and S2, respectively) as well as vibrissae motor cortex (M1), intermingled functional representations of touch, whisking, and licking were found, which partially re-organized during discrimination learning. These findings provide first glimpses of cortico-cortical communication but emphasize that for understanding the complete process of discrimination it will be crucial to elucidate the details of how neural processing is coordinated across brain-wide neuronal networks including the S1-S2-M1 triangle and cortical areas beyond.

Introduction

Sensory perception and discrimination are brain functions essential for animals in order to appropriately act and react in their environment. Depending on the sensory modality, particular physical features of the outside world are transduced into neuronal activity via specialized sensory receptors, for example the skin and hair follicle receptors transduce tactile information about the strength, direction, and frequency of touch-induced mechanical forces. In mammals, the action potential patterns generated in the periphery ascend via

*Present address: Department of Biology, Boston University, Boston, USA

synaptic relay stations in brainstem and thalamus, which act as spatiotemporal filters, and reach the neocortex as the highest loop of sensorimotor processing in the central nervous system. A prerequisite of sensory discrimination is stimulus perception, which requires the relevant neuronal populations to reach threshold for sufficient activation in order to enact appropriate behavioral responses. Neural correlates of encoding of stimulus intensity and perceptual learning have been investigated for decades (Mountcastle, 1993; Romo and Salinas, 2003) and a prime role in perception has been assigned to primary sensory areas in the neocortex, which exhibit a strong relationship between psychometric and neurometric curves (Romo and Salinas, 2003). Neural processing occurs in a spatially distributed fashion, though, and other cortical areas such as higher-order sensory areas, parietal association cortices, and frontal regions, have been implicated in stimulus representation and evaluation, too (Romo and de Lafuente, 2013; Romo et al., 2012). This is especially the case for more complex tasks that require discrimination of two or more stimuli in order to trigger different behavioral actions. How well stimuli can be discriminated depends on how different they are with respect to relevant features. Stimulus discriminability can be assessed experimentally by varying the similarity of the stimuli and measuring neurometric and psychometric curves of stimulus-difference representations. For example, the psychophysics of monkeys performing a vibrotactile discrimination task was found to be reflected well by the differences in neuronal firing rates in primary somatosensory cortex (S1) (Hernandez et al., 2000). Likewise, spike counts in barrel cortex neurons, integrated over a seconds time period, predicted well the performance of rats when they perceived pulsatile whisker stimuli (Gerdjikov et al., 2017).

In this review, rather than discussing neural correlates of perceptual detection thresholds and discrimination thresholds (for excellent reviews see (Diamond and Arabzadeh, 2013; Romo and de Lafuente, 2013; Romo and Salinas, 2003; Stuttgen et al., 2011), we focus on experimental conditions where animals are trained to discriminate two salient stimuli that are clearly perceived and easily distinguished in order to make an informed decision and initiate different behaviors. We will further focus on somatosensory discrimination of tactile stimuli, highlighting in particular the recent bout of studies that utilized novel whisker-based tasks for head-restrained mice. The rodent whisker-system has become a popular model system for studying tactile information processing due to is neuroethological relevance (Feldmeyer et al., 2013; Petersen, 2007). Previously, sensory discrimination has been studied largely in freely behaving rats, with animals engaging in specific tasks after initiating a trial with a nose poke; neural activity was often monitored by multi-unit or single-unit extracellular recordings and behavioral parameters concurrently extracted from high-speed videography (Krupa et al., 2004; Safaai et al., 2013; von Heimendahl et al., 2007). Compared to the large body of literature on discriminative behavior in other species as well as in freely behaving rodents, head-restrained experiments offer special opportunities because they enable the precise tracking of behavioral parameters such as whisker touch and movement as well as the application of intracellular recordings, calcium imaging techniques, and optogenetics to measure and manipulate the dynamic cortical representations from the cellular to the large network level. Importantly, the stability of head-fixed preparations enables to simultaneously record from a large population of neurons, from tens to hundreds of cells (Chen et al., 2013a; Harvey et al., 2012; O'Connor et al., 2013; Peron et al., 2015) to

a whole hemisphere (Ferezou et al., 2007; Mohajerani et al., 2013). In addition, when combined with specific labeling techniques, two-photon imaging in head-fixed animals allows the identification of distinct cell types during the experiment.

Several whisker-based discrimination tasks have been successfully set up for head-restrained rats or mice (Fig. 1) (Guo et al., 2014b). Habituation of rats or mice to the head-restraint condition usually takes a few days to a week (starting with brief episodes and then increasing the duration up to about an hour). Animals are then trained in different types of stimulus sampling: Either a single sample stimulus is perceived and its features compared to a previously (memorized) learned set of trained stimuli; or distinct locations of the stimulus rather than its specific features are of prime interest; or two stimuli applied in series are compared relative to each other (engaging some type of short-term memory); or two stimuli applied bilaterally at the same time need to be matched. One prominent task is ‘object localization’, where a pole is presented unilaterally to the vibrissae at different rostro-caudal positions and the animal is trained in go/no-go behavior for one target position versus distractor positions (Fig. 1A) (Huber et al., 2012; O'Connor et al., 2010a). In a different task the animal has to judge the roughness or smoothness of presented textures (typically sandpapers of different graininess) (Fig. 1B). For this ‘texture discrimination task’, the animal is trained by operant conditioning to associate one particular texture with reward delivery and to suppress licking upon presentation of non-target textures (often enforced through mild punishment, e.g., with unpleasant loud sound noise and/or time outs, i.e. delayed trial continuation) (Chen et al., 2013a; Chen et al., 2015). Moreover, a bilateral ‘two-alternative forced choice’ (2AFC) discrimination task has been established, where one whisker on each side is ‘wiggled’ at variable frequencies and the rat or mouse is trained to report, on which side the higher frequency occurs (Mayrhofer et al., 2013; Musall et al., 2014) (Fig. 1C). Finally, head-fixed mice free to navigate on a spherical treadmill use their whiskers can naturally track their position within a virtual corridor built by two opposing walls (Sofroniew et al., 2015) (Fig. 1D). Here, similar to an aperture-width discrimination task (Krupa et al., 2004), evaluation of the wall's position in terms of radial distance along the whisker length is required (Pammer et al., 2013). In contrast, in the pole localization task the object's position along the rostro-caudal (‘azimuthal’) axis is discriminated, for which active whisking plays a particular important role. Generally speaking, object localization and feature discrimination tasks, respectively, reflect the difference between the ‘where’ and ‘what’ aspects of sensory processing, which are thought to engage distinct areas and pathways within the larger-scale cortical circuit (Diamond et al., 2008).

Note that the distinction between sensory detection and discrimination tasks can become blurry. In detection tasks the animal simply has to detect the occurrence of a specific event, e.g. a particular mechanical stimulus that may or may not be predicted by other sensory cues (Kwon et al., 2016; Sachidhanandam et al., 2013). In contrast, in discrimination tasks one or several distractors (non-target stimuli) are applied (possibly also including stimulus omission). In both cases a representation of the target stimulus needs to be encoded and consolidated in memory during learning (with more or less details about object features and, if present, together with associated predictive cues). In subsequent trials, these memorized neural representations need to be retrieved and compared to current sensory stimuli in order to guide behavior. Animals may also learn to adapt their behavioral strategy to optimize

detection of the target stimulus, e.g. by restricting whisking to the expected target pole position, thus effectively turning a discrimination task into a ‘detection with distractors’ task (O'Connor et al., 2010a). In whisker-based tasks, licking for a liquid drop at a water spout as reward is often used to report the animal's decision (typically in combination with water scheduling to raise the animal's motivation and maximize the number of trials per experiment session). Discrimination tasks can also differ with respect to the required behavioral actions (Fig. 1): either the animal is conditioned to ‘go’ (lick) for a particular target stimulus but refrain from licking for any non-target (distractor) stimulus (so-called ‘go/no-go’ paradigm) or the animal is trained to lick at two different spouts (left/right) to indicate its decision among two possible choices, thus establishing a 2AFC paradigm (Mayrhofer et al., 2013). The advantage of 2AFC paradigms is that the level of task engagement (i.e., the attentional and motivational state of the animal) becomes apparent in the rate of ‘misses’, when the animal does not respond, whereas in the go/no-go paradigm correct rejections and misses are behaviorally not distinguishable.

In the following, we provide an overview of recent studies using head-restrained whisker-based discrimination tasks in mice to dissect the underlying neuronal pathways that contribute to sensorimotor processing. We focus on a few salient cortical areas and the communication between them, comprising primary and secondary somatosensory cortex (S1 and S2, respectively), primary motor cortex M1 (Fig. 1E). This sensorimotor ‘triangle’ is a key cortical network where each node (area) and edge (pathway) may differently contribute to sensory discrimination. Although these studies have allowed deeper insights into the larger-scale neural dynamics and communication among these regions, it is also clear that – depending on the specific task – further cortical areas (e.g. premotor areas M2 and ALM or PPC; Fig. 1E) as well as subcortical areas (e.g. thalamus or hippocampus) are involved in the different phases of sensory perception, stimulus evaluation, working memory, and motor control. Hence, this is a developing field, which can be expected to further expand in the coming years, especially in view of the continual improvements in experimental techniques.

S1 neuronal activity in whisker-based discrimination tasks

Whisker touches of objects vary in complexity depending on the type of task, the internal state of the mouse, and the object itself. ‘Where’ and ‘what’ aspects have been studied extensively in the rodent whisker system (Diamond et al., 2008), with ‘where’ referring to object position along the rostro-caudal (azimuthal), dorso-ventral (elevational), or radial (distance-from-body) axis. Originally designed for rats (Hill et al., 2008), the rostro-caudal pole localization task was adopted for head-restrained mice (Fig. 1A), first in a go/no-go paradigm (Chen et al., 2013a; Guo et al., 2014b; Huber et al.; O'Connor et al., 2010a), later as a 2AFC task (Guo et al., 2014a; Li et al., 2015). Animals in this task typically engage in active control of whisking, presumably to maximize the difference in touch-evoked responses between target and distractor locations (O'Connor et al., 2010a). In addition, rhythmic whisking may create a time reference signal, against which touch events from a single whisker can be compared across several seconds and aid in haptic perception (Knutsen et al., 2006; Mehta et al., 2007; O'Connor et al., 2010b). An active whisking strategy is also employed by mice in the texture discrimination task (Fig. 1B) (Chen et al., 2013a; Chen et al., 2015). A prominent feature of the physical whisker-sandpaper interaction

are so-called ‘stick-slip’ events, which occur when the whisker gets caught by a sandpaper grain, is stretched, and then released like a spring (Arabzadeh et al., 2005; Boubenec et al., 2012; Wolfe et al., 2008). The frequency of these stick-slip events is a key variable correlated with and thus encoding for graininess. Engaging in active whisking is beneficial for the animal as it increases the likelihood of stick-slip events in a texture dependent manner (Chen et al., 2015; von Heimendahl et al., 2007; Zuo et al., 2011). Hence, typical behavioral readout parameters in these tasks are whisking angle (for individual whiskers or averaged across multiple whiskers), whisker set point, contact-induced whisker curvature change, from which lateral and axial forces impinging on the whisker follicles can be estimated (Boubenec et al., 2012; O'Connor et al., 2010a; Pammer et al., 2013), and frequency of stick-slip events (Chen et al., 2015; von Heimendahl et al., 2007; Wolfe et al., 2008).

The representation of touch events in neuronal populations of S1 barrel cortex has been investigated using electrophysiological recordings or calcium imaging of touch-evoked neuronal responses in awake, behaving mice. Nowadays, many sensitive genetically encoded calcium indicators are available (reviewed in (Grienberger and Konnerth, 2012)). The results reported here were obtained with variants of either GCaMP6 (Chen et al., 2013b) or Yellow Cameleon (YC) (Horikawa et al., 2010); more recently, application of red-shifted calcium indicators also has become feasible (Bethge et al., 2017; Dana et al., 2016; Pilz et al., 2016). Despite variations among indicators regarding sensitivity, dynamic range, and kinetics, the fluorescence signals are commonly interpreted in terms of underlying firing rate changes. Whereas electrophysiological recordings can be targeted to neurons in all cortical layers, two-photon calcium imaging is, however, still easier to apply in supragranular layers compared to deep layers. In addition, AAV-induced expression schemes usually spare layer 4 (L4). Consequently, most calcium measurements in neocortex of behaving animals so far have been obtained from L2/3 neurons.

During object localization behavior, juxtacellular recordings revealed diverse responses across and within cortical layers (O'Connor et al., 2010a). Mean spike rates were larger, and a higher fraction of neurons active, in L4 and L5 compared to superficial L2/3, where neurons displayed relatively sparse activity. Response distributions within local neuronal populations were skewed, with only a small fraction of neurons contributing most of the spikes while the majority of neurons showed weaker responses. Two-photon calcium imaging in superficial L2/3 revealed distinct subsets of neurons that differed in their relationship to behavioral aspects such as whisking, touch, and licking (Peron et al., 2015). Active neurons can be functionally classified, for example based on how correlated their activity is with the whisking and touch variable, respectively (Chen et al., 2013a), or using generalized linear models (GLMs) with a set of behavioral variables as regressors (Peron et al., 2015). During object localization, some L2/3 neurons exhibited high correlation of their activity with one particular behavioral aspect (e.g. ‘whisking’ neurons) while others show mixed responses (Peron et al., 2015). Neurons from functionally distinct classes were spatially intermingled. A similar heterogeneity and intermingling of functional responses was also found in barrel cortex L2/3 neurons during the texture discrimination task (Chen et al., 2013a). In both studies around 40% of L2/3 neurons were active during the behavioral trials.

The functional diversity of neural responses in S1 may in part be attributed to the distinction between excitatory and inhibitory neurons. For example, identified GABAergic interneuron in L2/3 displayed a higher proportion of active neurons, especially of whisking neurons (Peron et al., 2015). Furthermore, in a whisker-stimulus detection task, functional characterization of different subtypes of GABAergic interneurons revealed cell-type-specific membrane potential dynamics and spike patterns (Sachidhanandam et al., 2016; Sachidhanandam et al., 2013). But even when considering only excitatory neurons, functional diversity remains. Could this heterogeneity reflect anatomical differences such as distinct connectivity to distant brain regions? For example, S1 gives rise to diverging projection pathways to S2 and M1 (Aronoff et al., 2010). Such cortico-cortical projection neurons are found in L2/3 as well as in infragranular layers (Aronoff et al., 2010; Chen et al., 2013a) and different types of neuronal pools with distinct projection targets can be identified in vivo with the help of retrograde tracer injections and two-photon microscopy (Chen et al., 2013a; Sato and Svoboda, 2010; Yamashita et al., 2013). Two-color retrograde labeling revealed that S1 L2/3 contains two largely non-overlapping, intermingled neuronal subsets, sending axonal projections to S2 (‘$S1_{S2}$ neurons’) and M1 (‘$S1_{M1}$ neurons’), respectively, and with only few neurons projecting to both S1 and M1 (Fig. 2A; usually a pool of unlabeled [UNL] neurons with undetermined projection targets remains). $S1_{S2}$ and $S1_{M1}$ projection neurons were shown to differ in their intrinsic electrophysiological properties in vivo (Yamashita et al., 2013). Two-photon calcium imaging of these neuronal pools revealed that they also differ regarding their functional response profiles during discrimination behaviors (Fig. 2B) (Chen et al., 2013a): Touch neurons were present in all anatomical classes, whereas whisking neurons generally were not found among $S1_{M1}$ neurons. The distribution of touch neurons across anatomical classes depended, however, on the specific behavioral task: A higher fraction of $S1_{M1}$ than $S1_{S2}$ neurons showed touch-related responses during object localization, whereas during texture discrimination a higher fraction of $S1_{S2}$ displayed touch-related activity compared to $S1_{M1}$ neurons (Fig. 2C) (Chen et al., 2013a). These results indicate that neuronal pools that give rise to specific projection pathways, participate in encoding multiple behavioral aspects and do so in a behavior-dependent manner.

Neuronal responses can be further analyzed by determining the discrimination power for distinguishing between particular trial types. For example, in the texture discrimination task some neurons were highly discriminative for Hit vs. CR trials, others discriminated between distinct non-target textures, and yet others were touch-responsive but showed poor discrimination power (Fig. 3A). Similarly, during object localization some neurons were highly discriminative for Hit vs. CR trials, others differentiated pole positions well, and further touch neurons were not discriminative at all (Fig. 3B) (Chen et al., 2013a). Thus, discrimination power appears non-homogeneously distributed in L2/3 neurons, which is consistent with earlier studies using electrophysiology (O'Connor et al., 2010b; Safaai et al., 2013; von Heimendahl et al., 2007). For individual neurons one can quantify the discrimination power and test whether it is significantly higher compared to chance level (usually tested by shuffling responses). Highly discriminative neurons typically are only a minority in the whole population, which covers the whole spectrum of discrimination power, from poor to high (Chen et al., 2013a; Peron et al., 2015). Does $S1_{S2}$ and $S1_{M1}$

discrimination power differ for specific tasks? Although discriminative neurons were found in both types of projection neurons for both behaviors, the fraction of discriminative neurons differed in a task-dependent manner: for texture discrimination a higher fraction of $S1_{S2}$ neurons compared to $S1_{M1}$ neurons showed significant Hit vs. CR discrimination power whereas the situation was reversed for object localization (Fig. 3C,D). In addition, in trials producing the same decision, $S1_{S2}$ neurons turned out to be better in discriminating texture type whereas $S1_{M1}$ neurons were better in discriminating object location (Chen et al., 2013a), consistent with the idea of emerging 'what' and 'where' processing streams. These findings imply that neurons in S1 encode information about object location, which they especially transmit to M1. Possibly, $S1_{M1}$ touch neurons integrate touch events with whisker position arriving from M1 feedback (see below). During texture discrimination, however, tactile information was carried less by $S1_{M1}$ neurons and forwarded largely to S2, indicating that cortical processing in this case may require higher-order sensory areas for evaluation of complex object features.

In summary, these results highlight the functional heterogeneity as well as the behavior-dependence of neuronal representations and discrimination power within the L2/3 neuronal population. Apparently, the S1 neuronal network adapts during learning to the task and adjusts information routing via its diverging projection pathways to S2 and M1 (see below). Behaviorally relevant touch events are represented in L2/3 of S1 in a sparse and distributed, heterogeneous and intermingled, as well as adaptive manner. The presence of whisking-related neurons in L2/3 of S1 makes it clear, however, that L2/3 neurons do not only process feedforward sensory information but also integrate information about behavioral variables such as self-motion. Such information could be partially conveyed through modulation of L4 neurons, which recently have been shown to transmit touch-related thalamocortical signals while suppressing whisking signals via feedforward local inhibition (Hires et al., 2015; Gutnisky et al., 2017). Nonetheless, the major sources of the extra information likely are the input pathways arriving in S1 from other cortical areas such as M1 and S2. We therefore take a closer look at these inter-areal communication pathways.

S1-M1 communication

Active sensing involves the communication between whisker-related S1 and M1. Whisker-related M1 is thought to participate in whisker movement control, but its exact influence on whisker movement – whether driving, suppressive, or initiating – is still being worked out (Ebbesen et al., 2017; Sreenivasan et al., 2016). Mice actively whisk to extract information about their close-by environment. S1 and M1 are reciprocally connected; whereas $S1_{M1}$ feed-forward projections are somatotopic (Aronoff et al., 2010; Kleinfeld et al., 2002; Mao et al., 2011) $M1_{S1}$ feedback projections are more diffusive (Aronoff et al., 2010; Veinante and Deschenes, 2003). Active exploration leads to object contacts, which produce sensory signals reaching S1 that are fed forward to M1 (Diamond et al., 2008; Ferezou et al., 2007; Petersen, 2007). This in return results in additional whisking to resample relevant objects. Feedback from M1 to S1 is thought to carry information about whisker position (Hill et al., 2011; Petreanu et al., 2012). Therefore both feedforward and feedback pathways may compose a dynamic processing loop to detect relevant objects in space (Sreenivasan et al.,

2016). As indicated above, the involvement of this S1-M1 loop in distinct types of tasks may differ.

By imaging L2/3 pyramidal neurons directly in M1, an intermingled representation of neurons with activity related to either touch, whisking or licking has been found (Huber et al., 2012). To study specifically the $M1_{S1}$ feedback projections, Petreanu et al. imaged axons projecting from M1 to L1 in S1 using two-photon imaging when mice performed an object localization task (Petreanu et al., 2012). Feedback information conveyed from M1 to S1 was diverse, encoding not only for whisker movement but also for touch and licking events. The importance of M1-to-S1 feedback was further demonstrated by imaging distal dendrites of L5 pyramidal neurons in S1, which elicited dendritic calcium signals when whiskers touched the pole at particular positions (Xu et al., 2012). These dendritic signals depended on M1 input, as they were abolished when M1 activity was blocked, and thus appear to integrate sensory input and M1 feedback. The integration of M1 feedback in S1 presumably is further shaped by polysynaptic circuit motifs involving inhibitory interneurons, such as the disinhibitory circuit implemented by VIP-expressing interneurons (Lee et al., 2013). Overall, these findings indicate that information related to touch, coming initially from the S1 feedforward projections, is relayed back to S1 possibly to reassure the touch. Interestingly, a subset of M1 neurons projecting back to S1 was sensitive to object location and displayed persistent activity that lasted for several seconds (Petreanu et al., 2012). This time window may allow past touch events to coincide with new incoming touch events and enable a continuous perception of object location within the loop. The presence of additional information that is not directly related to whiskers, e.g. licking, may hint to other areas affecting the S1-M1 loop, which we discuss further below.

S1-S2 communication

S1 and S2 also exhibit prominent reciprocal connectivity between areas. The functional role of S2 is poorly defined but may include multi-whisker processing and sensitivity to low-frequency modulation (Bokor et al., 2008; Melzer et al., 2006). Using tetrode recordings in freely behaving rats Zuo et al. found that in both S1 and S2 spike timing carries more information about texture stimuli and choice compared to spike rate (Zuo et al., 2015). Recently, the communication between these areas during sensory detection and discrimination has been studied using in vivo calcium imaging in head-fixed mice. One imaging study applied a special multi-area two-photon microscope, which enables simultaneous neuronal population imaging in S1 and S2 (Chen et al., 2016; Voigt et al., 2015). Several variants of such two-photon microscopes with enlarged field-of-view and multi-area imaging capability have been recently developed and are promising tools for studying inter-areal communication (Lecoq et al., 2014; Sofroniew et al., 2016; Stirman et al., 2016a). In addition, these multi-area measurements can be combined with retrograde labeling approaches to identify specific types of projection neurons (Fig. 4A). In this way, it becomes possible to analyze for the first time the coordination of neuronal population dynamics across two areas specifically for the mutually projecting neuronal pools (Fig. 4B). Simultaneous imaging of S1 and S2 neuronal populations during the discrimination task revealed coordinated patterns of activity between these areas, related to both motor behavior (whisking and licking) as well as sensory processing (Chen et al., 2016) (Fig. 4C,D).

Whereas motor-related activity patterns S1 and S2 appeared to mainly reflect common drive from other areas, possibly M1 or thalamic POm, the sensory- and decision-related activity patterns were found to be more specific to $S1_{S2}$ and $S2_{S1}$ neurons.

Another study used calcium imaging to measure the activity of axonal projections between S1 and S2 in a pole detection task (Fig. 4E) (Kwon et al., 2016). S2→S1 axons displayed movement-related activity during whisking and licking as well as choice-prominent activity, with larger responses in Hit trails compared to Miss trials (Fig. 4F,G). While it is unclear if choice-related activity is computed locally within S2 or inherited from elsewhere, choice-related activity observed in S1 was specifically inherited from S2 through cortico-cortical feedback ($S2_{S1}$) neurons. Moreover, feedforward ($S1_{S2}$) neurons showed stronger choice-related activity compared to other S1 neurons, suggesting that the transformation of sensory-related signal to choice-related signals involves a coordinated exchange of information between these specific types of cortico-cortical neurons (Fig. 4H). Taken together, these findings suggest that the cortico-cortical communication loop between S1 and S2 is dedicated to the processing and integration of sensory- and choice-related information.

Beyond the S1-S2-M1 triangle

These recent studies thus have begun to examine in much finer detail the information exchange occurring during specific behaviors within the highly interconnected S1-S2-M1 triangle. Whereas functional investigation of the direct pathways between S2 and M1 is still pending, further studies in head-fixed mice have targeted various cortical areas beyond the S1-S2-M1 triangle. In addition to M1, there may be other top-down effects from frontal cortex onto S1 that may be relevant for detection and discrimination of objects ((Gilbert and Sigman, 2007; Krupa et al., 2004; van Kerkoerle et al., 2017) for V1 of primates). One candidate area is the secondary motor area (M2), located medial to M1, which directly innervates whisker-related S1, S2 and M1. M2 projections onto sensory areas play a role in sensory discrimination in multiple modalities, e.g. vision (Zhang et al., 2014) or forelimb somato-sensation (Manita et al., 2015). In addition, M2 has been implicated in an adaptive sensorimotor task requiring mice to shift flexibly between multiple auditory-motor mappings (Siniscalchi et al., 2016). Thus goal-directed strategies may be fed back from M2 to S1 in order to emphasize or attenuate incoming sensory input.

In order to better understand the interactions of higher-order cortical areas with lower-order sensory areas mice can be trained to withhold their report for several seconds (Guo et al., 2014a). Thus, information encoded within whisker-related loops (i.e. S1-S2 and S1-M1) may be re-routed to other areas. The anterior lateral motor cortex (ALM) has been found to play a role in planning and executing movement during an object detection task (Guo et al., 2014a; Li et al., 2015). Interestingly, recent experiments demonstrate that persistent activity in ALM during movement preparation requires concerted activation of thalamic regions (Guo et al., 2017), indicating that an excitatory cross-regional loop encompassing cortical and sub-cortical regions is required for holding relevant information. For object discrimination it is less clear whether ALM directly affects S1 or how it may be involved in such a task. It is possible that unlike in an object detection task, different areas could participate in maintaining information for object discrimination. In this context, M2 as

higher-order motor area could possibly be recruited to hold information about movement preparation before initiating goal-directed action. In addition, posterior cortical areas, e.g. PPC, could participate in reverberating activity during the delay period. Further imaging studies focusing on activity patterns in these other cortical areas during head-fixed behaviors will be required to obtain a more complete picture of cortical signal flow during sensory discrimination and movement preparation. In addition, information exchange with subcortical regions such as thalamus, hippocampus, and striatum, is likely to be important, especially during task learning.

Circuit Reorganization during Learning

Whether signal flow patterns between cortical areas are built into the system and called upon in a behavior-dependent manner, or whether they are learned during the acquisition of a behavioral task, is an open question. Some indication of the underlying process has been revealed by chronic imaging of neuronal activity during task learning (Fig. 5). Here, the ability to consistently find the same cells under the two-photon microscope again and again over days to weeks – using anatomical landmarks such as blood vessel pattern and neuronal cell body constellations (Margolis et al., 2012) – is a crucial advantage. Such chronic measurements meanwhile have become routine practice.

For texture discrimination, mice typically develop an active whisking strategy during the training period (Fig. 5A), presumably optimizing the gathering of touch-induced information relevant for discrimination, such as stick-slip events or curvature changes (Chen et al., 2015). While individual neurons generally exhibited some session-to-session variability, additional $S1_{M1}$ neurons became responsive to whisker touch during training (Fig. 5B,C), suggesting increased involvement in sensory processing (Chen et al., 2015). However, they maintained their encoding for basic stimulus features such as the frequency of stick-slip events or the maximal change in whisker curvature. These results suggest that this pathway mainly serves to faithfully represent incoming sensory information and that the recruitment of additional $S1_{M1}$ touch neurons could simply reflect recognition of the heightened relevance of whisker touches. Correspondingly, neurons in vibrissal M1 were also found to become more responsive during the whisker sampling period in the pole detection task (Huber et al., 2012). In this study, a shift in the temporal structure of activity was also observed, with neurons firing earlier during the whisking-sampling period. This could be partly explained by altered behavior as mice started to whisk more concentrated when sampling the pole position. Hence, the S1-M1 loop seems to become more engaged during learning of whisker-based tactile discriminations, likely participating in the development of a suitable motor strategy as well as enhancing the saliency of key stimulus parameters to facilitate collection of decision-relevant information.

In the other major pathway from S1 to S2 a different picture emerged. In contrast to $S1_{M1}$ neurons, $S1_{S2}$ neurons exhibited altered sensory responses, acquiring decision-related activity over the course of training (Chen et al., 2015). Whereas the fraction of $S1_{S2}$ touch neurons remained constant (Fig. 5C), a much larger reorganization within the $S1_{S2}$ neuronal pool took place, so that after learning a largely different subset of $S1_{S2}$ neurons was active during touch compared to the active subset before training. In addition, non-touch $S1_{S2}$

neurons were increasingly suppressed when the animals were engaged in the task. During learning a larger fraction of $S1_{S2}$ touch neurons became able to discriminate go and no-go trials and the discrimination power of discriminating neurons increased (Fig. 5D). These findings demonstrate that learning has the potential to alter communication between cortical areas in two manners, either by strengthening the information flow in the loop between areas, or by altering the content of information exchanged between areas.

Another study investigated the representation of touch neurons and whisking neurons during object localization across large parts of a cortical column in the barrel cortex (Fig. 5E) (Peron et al., 2015). A subset of neurons was repeatedly imaged during training until the animal reached expert performance (Fig. 5F). About 15% of L2/3 showed touch-related activity and this fraction stayed constant across the entire training period (Fig. 5G). The percentage of whisking neurons was also between 10-30% and increased early during training. This change likely reflected changes in movement strategy, however, rather than indicating neural plasticity. Although the fraction of touch neurons is in the same range as observed for texture discrimination (Chen et al., 2015), the results are difficult to compare because no distinction between different types of projection neurons was made in the Peron et al. study. Since only few whisking neurons were found in the Chen et al. study they were not separately analyzed. Interestingly, whereas neurometric performance remained flat during training, psychometric performance increased (Peron et al., 2015), suggesting that suitable S1 representation of tactile information is always present but more effectively processed during learning.

These early studies on learning-associated changes in S1 neuronal representations thus indicate that functional sub-networks are relatively stable in size, albeit individual neurons exhibit some baseline variability, and that intricate changes in representation can occur selectively in the $S1_{S2}$ projection neuron subset, perhaps when feature information needs to be exchanged with S2 and related to the animal's choice behavior.

Conclusions and Outlook

In summary, the application of modern imaging methods in head-fixed mice performing various behavioral tasks has been transformative by enabling researchers to address old questions about neural correlates of behavior with a fresh perspective. The combination of neural tracing methods to identify specific subsets of neurons with calcium imaging has proven particularly powerful as it allows the functional analysis of local pools of neurons whose projection target area is known. In the past, such experiments were extremely difficult using electrophysiological methods. For example, in previous monkey studies recording from different areas (Bastos et al., 2015; Romo and de Lafuente, 2013; Siegel et al., 2015) it was not possible to dissect the neuronal population from each area into different projections, cell types, or even layer specificity. In these studies the flow of information was implied by latency differences or rhythmic synchronization between areas but not directly shown. The new approaches now feasible in rodents enabled first insights into the true information transfer between cortical areas.

We have reviewed here in particular studies using different whisker-based head-fixed tasks that dissect the S1-S2-M1 triangle into its nodes (areas) and edges (pathways). Measuring neuronal responses within each node itself (e.g. in the S1 population) showed heterogeneous encoding of different behavioral parameters. Measuring only from a subset of the population (e.g. projections to a specific area) could extract, however, more behavior-specific information. For example, the S1-M1 loop carries information mainly in motor-related tasks that are thought to engage “where” pathways. In contrast, the S1-S2 loop carries information mainly related to sensory-related tasks, likely representing “what” pathways. Such dissections are very important for understanding not only how the brain discriminates between two stimuli, but also in investigating other higher-order function such as perception, attention and working memory. In this context, such pathway-specific measurements should be ‘copied’ to other brain areas and pathways to better understand information flow during behavior.

Further progress will likely occur along multiple lines: First, head-fixed behavioral paradigms will further expand, encompassing discrimination in the auditory and visual modalities, even involving touch-screen based perception tasks (Stirman et al., 2016b), as well as higher cognitive tasks. Similar approaches are also already applied in other species, for example in head-fixed flies (Kim et al., 2017) and stabilized larval zebrafish (Ahrens et al., 2012). Second, the rapid expansion of imaging technologies enabling simultaneous imaging from large field-of-views or across many areas (Chen et al., 2016; Lecoq et al., 2014; Sofroniew et al., 2016; Stirman et al., 2016a) will continue and enable collection of comprehensive data sets of neuronal network representations and neuronal pathway dynamics. Third, new transgenic mouse lines expressing sensitive calcium indicators (Dana et al., 2014; Madisen et al., 2015) (Bethge et al., 2017) will further facilitate functional imaging of defined subsets of neurons, applied alone or in combination with viral vectors. Fourth, improved microscopy techniques, including holographic methods (Yang et al., 2016) and 3-photon microscopy with novel laser types (Ouzounov et al., 2017), as well as recent advances in the in vivo application of red-shifted calcium indicators (Dana et al., 2016) (Bethge et al., 2017) should enable similar calcium imaging studies in deeper cortical layers, including L6. Data sets covering large field-of-views and all cortical layers will be highly suitable for scrutinizing high-dimensional population dynamics and comparing experimental results to large-scale computational network models. Fifth, manipulative tools such as optogenetics or chemogenetics will be increasingly applied to test hypotheses on exactly what information is transferred along specific neuronal pathways. Finally, neuronal subtypes will be further dissected using modern genetic techniques, regarding both long-range projections as well as local circuit motifs, especially involving the action of specific GABAergic interneuron subtypes. Taken together, these powerful new approaches promise new leaps in our understanding of the principles of neural circuit dynamics. Thus, exciting times lie ahead of us.

Acknowledgments

Work by the author's presented in this review was supported by the University of Zurich, the Swiss National Science Foundation (grants 310030-127091 and 31003A_149858; F.H.), the US BRAIN Initiative (NIH grant 1U01NS090475-01, F.H.), a Forschungskredit of the University of Zurich (grant 541541808, J.L.C.) and a fellowship from the US National Science Foundation, International Research Fellowship Program (grant 1158914,

J.L.C.). We also acknowledge support by an ERC Advanced Grant (670757 BRAINCOMPATH; F.H.) and an EMBO postdoctoral fellowship (A.G.).

References

Ahrens MB, Li JM, Orger MB, Robson DN, Schier AF, Engert F, Portugues R. Brain-wide neuronal dynamics during motor adaptation in zebrafish. Nature. 2012; 485:471–U480. [PubMed: 22622571]

Arabzadeh E, Zorzin E, Diamond ME. Neuronal encoding of texture in the whisker sensory pathway. PLoS Biol. 2005; 3:e17. [PubMed: 15660157]

Aronoff R, Matyas F, Mateo C, Ciron C, Schneider B, Petersen CC. Long-range connectivity of mouse primary somatosensory barrel cortex. Eur J Neurosci. 2010; 31:2221–2233. [PubMed: 20550566]

Bastos AM, Vezoli J, Bosman CA, Schoffelen JM, Oostenveld R, Dowdall JR, De Weerd P, Kennedy H, Fries P. Visual areas exert feedforward and feedback influences through distinct frequency channels. Neuron. 2015; 85:390–401. [PubMed: 25556836]

Bethge P, Carta S, Lorenzo DA, Egolf L, Goniotaki D, Madisen L, Voigt FF, Chen JL, Schneider B, Ohkura M, et al. An R-CaMP1.07 reporter mouse for cell-type-specific expression of a sensitive red fluorescent calcium indicator. PLoS One. 2017; 12:e0179460. [PubMed: 28640817]

Bokor H, Acsady L, Deschenes M. Vibrissal responses of thalamic cells that project to the septal columns of the barrel cortex and to the second somatosensory area. J Neurosci. 2008; 28:5169–5177. [PubMed: 18480273]

Boubenec Y, Shulz DE, Debregeas G. Whisker encoding of mechanical events during active tactile exploration. Front Behav Neurosci. 2012; 6:74. [PubMed: 23133410]

Chen JL, Carta S, Soldado-Magraner J, Schneider BL, Helmchen F. Behaviour-dependent recruitment of long-range projection neurons in somatosensory cortex. Nature. 2013a; 499:336–340. [PubMed: 23792559]

Chen JL, Margolis DJ, Stankov A, Sumanovski LT, Schneider BL, Helmchen F. Pathway-specific reorganization of projection neurons in somatosensory cortex during learning. Nat Neurosci. 2015; 18:1101–1108. [PubMed: 26098757]

Chen JL, Voigt FF, Javadzadeh M, Krueppel R, Helmchen F. Long-range population dynamics of anatomically defined neocortical networks. Elife. 2016; 5:e14679. [PubMed: 27218452]

Chen TW, Wardill TJ, Sun Y, Pulver SR, Renninger SL, Baohan A, Schreiter ER, Kerr RA, Orger MB, Jayaraman V, et al. Ultrasensitive fluorescent proteins for imaging neuronal activity. Nature. 2013b; 499:295–300. [PubMed: 23868258]

Dana H, Chen TW, Hu A, Shields BC, Guo C, Looger LL, Kim DS, Svoboda K. Thy1-GCaMP6 transgenic mice for neuronal population imaging in vivo. PLoS One. 2014; 9:e108697. [PubMed: 25250714]

Dana H, Mohar B, Sun Y, Narayan S, Gordus A, Hasseman JP, Tsegaye G, Holt GT, Hu A, Walpita D, et al. Sensitive red protein calcium indicators for imaging neural activity. Elife. 2016; 5:e12727. [PubMed: 27011354]

Diamond ME, Arabzadeh E. Whisker sensory system - from receptor to decision. Prog Neurobiol. 2013; 103:28–40. [PubMed: 22683381]

Diamond ME, von Heimendahl M, Knutsen PM, Kleinfeld D, Ahissar E. 'Where' and 'what' in the whisker sensorimotor system. Nat Rev Neurosci. 2008; 9:601–612. [PubMed: 18641667]

Ebbesen CL, Doron G, Lenschow C, Brecht M. Vibrissa motor cortex activity suppresses contralateral whisking behavior. Nat Neurosci. 2017; 20:82–89. [PubMed: 27798633]

Feldmeyer D, Brecht M, Helmchen F, Petersen CCH, Poulet JFA, Staiger JF, Luhmann HJ, Schwarz C. Barrel cortex function. Progress in Neurobiology. 2013; 103:3–27. [PubMed: 23195880]

Ferezou I, Haiss F, Gentet LJ, Aronoff R, Weber B, Petersen CC. Spatiotemporal dynamics of cortical sensorimotor integration in behaving mice. Neuron. 2007; 56:907–923. [PubMed: 18054865]

Gerdjikov TV, Bergner CG, Schwarz C. Global tactile coding in rat barrel cortex in the absence of local cues. Cereb Cortex. 2017 May.11:1–13.

Gilbert CD, Sigman M. Brain states: top-down influences in sensory processing. Neuron. 2007; 54:677–696. [PubMed: 17553419]

Grienberger C, Konnerth A. Imaging calcium in neurons. Neuron. 2012; 73:862–885. [PubMed: 22405199]

Guo ZCV, Li N, Huber D, Ophir E, Gutnisky D, Ting JT, Feng GP, Svoboda K. Flow of Cortical Activity Underlying a Tactile Decision in Mice. Neuron. 2014a; 81:179–194. [PubMed: 24361077]

Guo ZV, Hires SA, Li N, O'Connor DH, Komiyama T, Ophir E, Huber D, Bonardi C, Morandell K, Gutnisky D, et al. Procedures for behavioral experiments in head-fixed mice. PLoS One. 2014b; 9:e88678. [PubMed: 24520413]

Guo ZV, Inagaki HK, Daie K, Druckmann S, Gerfen CR, Svoboda K. Maintenance of persistent activity in a frontal thalamocortical loop. Nature. 2017; 545:181–186. [PubMed: 28467817]

Gutnisky DA, Yu J, Hires SA, To MS, Bale MR, Svoboda K, Golomb D. Mechanisms underlying a thalamocortical transformation during active tactile sensation. Plos Comput Biol. 2017; 13:e1005576. [PubMed: 28591219]

Harvey CD, Coen P, Tank DW. Choice-specific sequences in parietal cortex during a virtual-navigation decision task. Nature. 2012; 484:62–68. [PubMed: 22419153]

Hernandez A, Zainos A, Romo R. Neuronal correlates of sensory discrimination in the somatosensory cortex. Proc Natl Acad Sci U S A. 2000; 97:6191–6196. [PubMed: 10811922]

Hill DN, Bermejo R, Zeigler HP, Kleinfeld D. Biomechanics of the vibrissa motor plant in rat: rhythmic whisking consists of triphasic neuromuscular activity. J Neurosci. 2008; 28:3438–3455. [PubMed: 18367610]

Hill DN, Curtis JC, Moore JD, Kleinfeld D. Primary motor cortex reports efferent control of vibrissa motion on multiple timescales. Neuron. 2011; 72:344–356. [PubMed: 22017992]

Hires SA, Gutnisky DA, Yu J, O'Connor DH, Svoboda K. Low-noise encoding of active touch by layer 4 in the somatosensory cortex. Elife. 2015; 4

Horikawa K, Yamada Y, Matsuda T, Kobayashi K, Hashimoto M, Matsu-ura T, Miyawaki A, Michikawa T, Mikoshiba K, Nagai T. Spontaneous network activity visualized by ultrasensitive Ca^{2+} indicators, yellow Cameleon-Nano. Nature Methods. 2010; 7:729–732. [PubMed: 20693999]

Huber D, Gutnisky DA, Peron S, O'Connor DH, Wiegert JS, Tian L, Oertner TG, Looger LL, Svoboda K. Multiple dynamic representations in the motor cortex during sensorimotor learning. Nature. 2012; 484:473–478. [PubMed: 22538608]

Kim SS, Rouault H, Druckmann S, Jayaraman V. Ring attractor dynamics in the Drosophila central brain. Science. 2017; 356:849–853. [PubMed: 28473639]

Kleinfeld D, Sachdev RN, Merchant LM, Jarvis MR, Ebner FF. Adaptive filtering of vibrissa input in motor cortex of rat. Neuron. 2002; 34:1021–1034. [PubMed: 12086648]

Knutsen PM, Pietr M, Ahissar E. Haptic object localization in the vibrissal system: behavior and performance. J Neurosci. 2006; 26:8451–8464. [PubMed: 16914670]

Krupa DJ, Wiest MC, Shuler MG, Laubach M, Nicolelis MA. Layer-specific somatosensory cortical activation during active tactile discrimination. Science. 2004; 304:1989–1992. [PubMed: 15218154]

Kwon SE, Yang H, Minamisawa G, O'Connor DH. Sensory and decision-related activity propagate in a cortical feedback loop during touch perception. Nat Neurosci. 2016; 19:1243–1249. [PubMed: 27437910]

Lecoq J, Savall J, Vucinic D, Grewe BF, Kim H, Li JZ, Kitch LJ, Schnitzer MJ. Visualizing mammalian brain area interactions by dual-axis two-photon calcium imaging. Nat Neurosci. 2014; 17:1825–1829. [PubMed: 25402858]

Lee S, Kruglikov I, Huang ZJ, Fishell G, Rudy B. A disinhibitory circuit mediates motor integration in the somatosensory cortex. Nat Neurosci. 2013; 16:1662–1670. [PubMed: 24097044]

Li N, Chen TW, Guo ZV, Gerfen CR, Svoboda K. A motor cortex circuit for motor planning and movement. Nature. 2015; 519:51–56. [PubMed: 25731172]

Madisen L, Garner AR, Shimaoka D, Chuong AS, Klapoetke NC, Li L, van der Bourg A, Niino Y, Egolf L, Monetti C, et al. Transgenic mice for intersectional targeting of neural sensors and effectors with high specificity and performance. Neuron. 2015; 85:942–958. [PubMed: 25741722]

Manita S, Suzuki T, Homma C, Matsumoto T, Odagawa M, Yamada K, Ota K, Matsubara C, Inutsuka A, Sato M, et al. A Top-Down Cortical Circuit for Accurate Sensory Perception. Neuron. 2015; 86:1304–1316. [PubMed: 26004915]

Mao T, Kusefoglu D, Hooks BM, Huber D, Petreanu L, Svoboda K. Long-range neuronal circuits underlying the interaction between sensory and motor cortex. Neuron. 2011; 72:111–123. [PubMed: 21982373]

Margolis DJ, Lütcke H, Schulz K, Haiss F, Weber B, Kugler S, Hasan MT, Helmchen F. Reorganization of cortical population activity imaged throughout long-term sensory deprivation. Nature Neuroscience. 2012; 15:1539–1546. [PubMed: 23086335]

Mayrhofer JM, Skreb V, von der Behrens W, Musall S, Weber B, Haiss F. Novel two-alternative forced choice paradigm for bilateral vibrotactile whisker frequency discrimination in head-fixed mice and rats. Journal of Neurophysiology. 2013; 109:273–284. [PubMed: 23054598]

Mehta SB, Whitmer D, Figueroa R, Williams BA, Kleinfeld D. Active spatial perception in the vibrissa scanning sensorimotor system. PLoS Biol. 2007; 5:e15. [PubMed: 17227143]

Melzer P, Champney GC, Maguire MJ, Ebner FF. Rate code and temporal code for frequency of whisker stimulation in rat primary and secondary somatic sensory cortex. Exp Brain Res. 2006; 172:370–386. [PubMed: 16456683]

Mohajerani MH, Chan AW, Mohsenvand M, LeDue J, Liu R, McVea DA, Boyd JD, Wang YT, Reimers M, Murphy TH. Spontaneous cortical activity alternates between motifs defined by regional axonal projections. Nature Neuroscience. 2013; 16:1426–1435. [PubMed: 23974708]

Mountcastle VB. Temporal order determinants in a somesthetic frequency discrimination: sequential order coding. Ann N Y Acad Sci. 1993; 682:150–170. [PubMed: 8323110]

Musall S, von der Behrens W, Mayrhofer JM, Weber B, Helmchen F, Haiss F. Tactile frequency discrimination is enhanced by circumventing neocortical adaptation. Nature Neuroscience. 2014; 17(11):1567–73. [PubMed: 25242306]

O'Connor DH, Clack NG, Huber D, Komiyama T, Myers EW, Svoboda K. Vibrissa-based object localization in head-fixed mice. Journal of Neuroscience. 2010a; 30:1947–1967. [PubMed: 20130203]

O'Connor DH, Hires SA, Guo ZV, Li N, Yu J, Sun QQ, Huber D, Svoboda K. Neural coding during active somatosensation revealed using illusory touch. Nature Neuroscience. 2013; 16:958–965. [PubMed: 23727820]

O'Connor DH, Peron SP, Huber D, Svoboda K. Neural activity in barrel cortex underlying vibrissa-based object localization in mice. Neuron. 2010b; 67:1048–1061. [PubMed: 20869600]

Ouzounov DG, Wang T, Wang M, Feng DD, Horton NG, Cruz-Hernandez JC, Cheng YT, Reimer J, Tolias AS, Nishimura N, et al. In vivo three-photon imaging of activity of GCaMP6-labeled neurons deep in intact mouse brain. Nat Methods. 2017; 14:388–390. [PubMed: 28218900]

Pammer L, O'Connor DH, Hires SA, Clack NG, Huber D, Myers EW, Svoboda K. The mechanical variables underlying object localization along the axis of the whisker. Journal of Neuroscience. 2013; 33:6726–6741. [PubMed: 23595731]

Peron SP, Freeman J, Iyer V, Guo C, Svoboda K. A cellular resolution map of barrel cortex activity during tactile behavior. Neuron. 2015; 86:783–799. [PubMed: 25913859]

Petersen CC. The functional organization of the barrel cortex. Neuron. 2007; 56:339–355. [PubMed: 17964250]

Petreanu L, Gutnisky DA, Huber D, Xu NL, O'Connor DH, Tian L, Looger L, Svoboda K. Activity in motor-sensory projections reveals distributed coding in somatosensation. Nature. 2012; 489:299–303. [PubMed: 22922646]

Pilz GA, Carta S, Stauble A, Ayaz A, Jessberger S, Helmchen F. Functional imaging of dentate granule cells in the adult mouse hippocampus. Journal of Neuroscience. 2016; 36:7407–7414. [PubMed: 27413151]

Romo R, de Lafuente V. Conversion of sensory signals into perceptual decisions. Prog Neurobiol. 2013; 103:41–75. [PubMed: 22472964]

Romo R, Lemus L, de Lafuente V. Sense, memory, and decision-making in the somatosensory cortical network. Current Opinion in Neurobiology. 2012; 22:914–919. [PubMed: 22939031]

Romo R, Salinas E. Flutter discrimination: neural codes, perception, memory and decision making. Nat Rev Neurosci. 2003; 4:203–218. [PubMed: 12612633]

Sachidhanandam S, Sermet BS, Petersen CC. Parvalbumin-expressing GABAergic neurons in mouse barrel cortex contribute to gating a goal-directed sensorimotor transformation. Cell Reports. 2016; (16):S2211–1247. 30334–5.

Sachidhanandam S, Sreenivasan V, Kyriakatos A, Kremer Y, Petersen CCH. Membrane potential correlates of sensory perception in mouse barrel cortex. Nature Neuroscience. 2013; 16:1671–1677. [PubMed: 24097038]

Safaai H, von Heimendahl M, Sorando JM, Diamond ME, Maravall M. Coordinated population activity underlying texture discrimination in rat barrel cortex. J Neurosci. 2013; 33:5843–5855. [PubMed: 23536096]

Sato TR, Svoboda K. The functional properties of barrel cortex neurons projecting to the primary motor cortex. J Neurosci. 2010; 30:4256–4260. [PubMed: 20335461]

Siegel M, Buschman TJ, Miller EK. Cortical information flow during flexible sensorimotor decisions. Science. 2015; 348:1352–1355. [PubMed: 26089513]

Siniscalchi MJ, Phoumthipphavong V, Ali F, Lozano M, Kwan AC. Fast and slow transitions in frontal ensemble activity during flexible sensorimotor behavior. Nat Neurosci. 2016; 19:1234–1242. [PubMed: 27399844]

Sofroniew NJ, Flickinger D, King J, Svoboda K. A large field of view two-photon mesoscope with subcellular resolution for in vivo imaging. Elife. 2016; 5:e14472. [PubMed: 27300105]

Sofroniew NJ, Vlasov YA, Hires SA, Freeman J, Svoboda K. Neural coding in barrel cortex during whisker-guided locomotion. Elife. 2015; 4:e12559. [PubMed: 26701910]

Sreenivasan V, Esmaeili V, Kiritani T, Galan K, Crochet S, Petersen CC. Movement initiation signals in mouse whisker motor cortex. Neuron. 2016; 92:1368–1382. [PubMed: 28009277]

Stirman JN, Smith IT, Kudenov MW, Smith SL. Wide field-of-view, multi-region, two-photon imaging of neuronal activity in the mammalian brain. Nat Biotechnol. 2016a; 34:857–862. [PubMed: 27347754]

Stirman JN, Townsend LB, Smith SL. A touchscreen based global motion perception task for mice. Vision Res. 2016b; 127:74–83. [PubMed: 27497283]

Stuttgen MC, Schwarz C, Jakel F. Mapping spikes to sensations. Front Neurosci. 2011; 5:125. [PubMed: 22084627]

van Kerkoerle T, Self MW, Roelfsema PR. Layer-specificity in the effects of attention and working memory on activity in primary visual cortex. Nat Commun. 2017; 8:13804. [PubMed: 28054544]

Veinante P, Deschenes M. Single-cell study of motor cortex projections to the barrel field in rats. J Comp Neurol. 2003; 464:98–103. [PubMed: 12866130]

Voigt FF, Chen JL, Kruppel R, Helmchen F. A modular two-photon microscope for simultaneous imaging of distant cortical areas in vivo. SPIE Conference, Multiphoton Microscopy in the Biomedical Sciences XV Book Series: Proceedings of SPIE. 2015; 9329 Article Number: 93292C.

von Heimendahl M, Itskov PM, Arabzadeh E, Diamond ME. Neuronal activity in rat barrel cortex underlying texture discrimination. PLoS Biol. 2007; 5:e305. [PubMed: 18001152]

Wolfe J, Hill DN, Pahlavan S, Drew PJ, Kleinfeld D, Feldman DE. Texture coding in the rat whisker system: slip-stick versus differential resonance. PLoS Biology. 2008; 6:e215. [PubMed: 18752354]

Xu NL, Harnett MT, Williams SR, Huber D, O'Connor DH, Svoboda K, Magee JC. Nonlinear dendritic integration of sensory and motor input during an active sensing task. Nature. 2012; 492:247–251. [PubMed: 23143335]

Yamashita T, Pala A, Pedrido L, Kremer Y, Welker E, Petersen CC. Membrane potential dynamics of neocortical projection neurons driving target-specific signals. Neuron. 2013; 80:1477–1490. [PubMed: 24360548]

Yang W, Miller JE, Carrillo-Reid L, Pnevmatikakis E, Paninski L, Yuste R, Peterka DS. Simultaneous Multi-plane Imaging of Neural Circuits. Neuron. 2016; 89:269–284. [PubMed: 26774159]

Zhang SY, Xu M, Kamigaki T, Do JPH, Chang WC, Jenvay S, Miyamichi K, Luo LQ, Dan Y. SELECTIVE ATTENTION Long-range and local circuits for top-down modulation of visual cortex processing. Science. 2014; 345:660–665. [PubMed: 25104383]

Zuo Y, Perkon I, Diamond ME. Whisking and whisker kinematics during a texture classification task. Philosophical transactions of the Royal Society of London Series B, Biological Sciences. 2011; 366:3058–3069. [PubMed: 21969687]

Zuo Y, Safaai H, Notaro G, Mazzoni A, Panzeri S, Diamond ME. Complementary contributions of spike timing and spike rate to perceptual decisions in rat S1 and S2 cortex. Current Biology. 2015; 25:357–363. [PubMed: 25619766]

Highlights

- We review studies of neuronal activity in mouse barrel cortex and connected cortical areas during tactile behavioral tasks.
- Two-photon calcium imaging revealed diverse and behavior-dependent neuronal activities in S1 and the S1-S2 and S1-M1 loops.
- Segregation in anatomically distinct projection pathways uncovered pathway-specific modifications during learning.
- These approaches promise further dissection of behavior-related activity in local cortical circuits and cortico-cortical pathways.

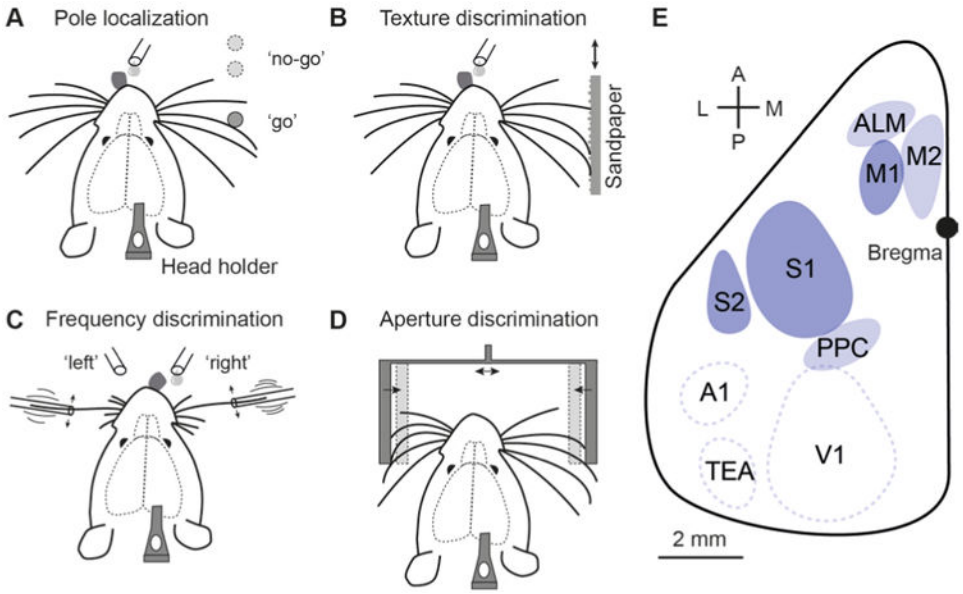

Figure 1.

Different types of whisker-based tactile discrimination tasks that have been established in head-restrained rodents. (A) Object localization. The animal needs to judge the position of a vertical pole. (B) Texture discrimination. The roughness of sandpaper presented to the whiskers has to be evaluated. (C) Bilateral frequency discrimination task. The animal has to compare the two stimulation frequencies on both sides. (D) Aperture discrimination. The width and centrality of the aperture have to be evaluated. (E) Schematic top view on the left hemisphere of mouse neocortex indicating several key areas for whisker-based discrimination behavior. S1: primary somatosensory cortex (barrel field), S2: secondary somatosensory cortex, M1: primary motor cortex, M2: secondary motor cortex, ALM: anterior lateral motor area, PPC: posterior parietal cortex; also indicated are A1: primary auditory cortex, V1: primary visual cortex, and TEa: temporal association area.

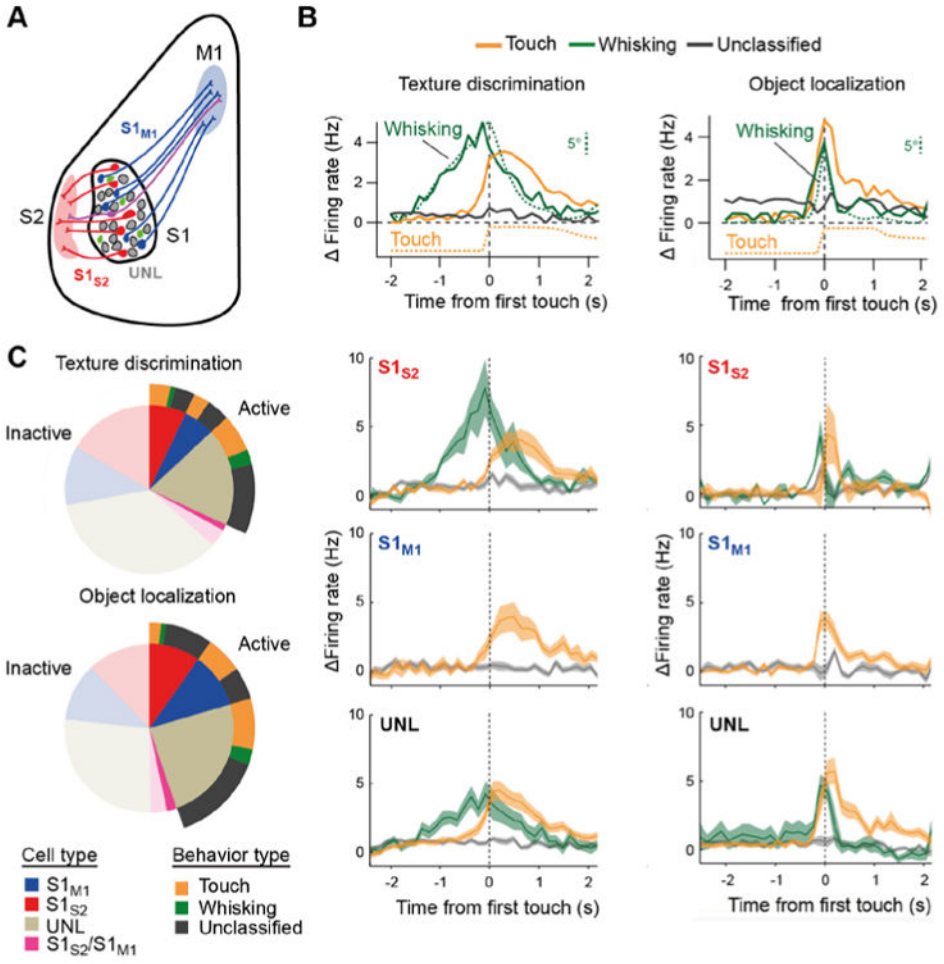

Figure 2.

Classification of neuronal responses in S1. (A) Schematic illustration of the retrograde labeling strategies for anatomical segregation of specific projection pathways, here the S2-projecting ($S1_{S2}$, red) and M1-projecting ($S1_{M1}$, blue) pathways, respectively. UNL denote 'unlabeled' neurons with unspecified projection targets. Green neurons indicate additional local interneurons. Two-photon calcium imaging was performed on L2/3 neurons that expressed YC-Nano140 as sensitive calcium indicator. For each neuron instantaneous firing rate changes were obtained by deconvolution of the YC-Nano140 calcium signals. (B) Top: Relative change in mean firing rate over the trial period aligned to first touch (dashed line) for neurons functionally classified into 'Whisking', 'Touch', and 'Unclassified' neurons (average across all neurons in each class). In addition, whisking is shown as the mean envelope of whisking amplitude, which was calculated as the difference between maximum and minimum whisker angles along a sliding window equal to the imaging frame duration (142 ms). The touch variable indicates the likelihood of the principal whisker to be in contact with the texture, obtained by averaging binary touch vectors across trials. Whisking and touch analyses were performed through visual inspection of high-speed videos. Note the correspondence between the time course of whisking amplitude and firing rate change in whisking neurons and between touch onset and the activation of touch neurons. Lower panels: Same data subdivided into the three anatomically defined subpopulations of $S1_{S2}$,

$S1_{M1}$, and UNL neurons, respectively. Traces represent averages across all neurons for each class (shaded area, s.e.m.). Panels in the left column refer to texture discrimination behavior, panels in the right column to object localization. (C) Distribution of imaged active neurons according to cell type and behaviour classification for texture discrimination (top) and object localization (bottom) behavior. For completeness 'inactive' neurons not showing significant activity during the behavior sessions are also depicted (transparent areas). All panels adapted from (Chen et al., 2013a).

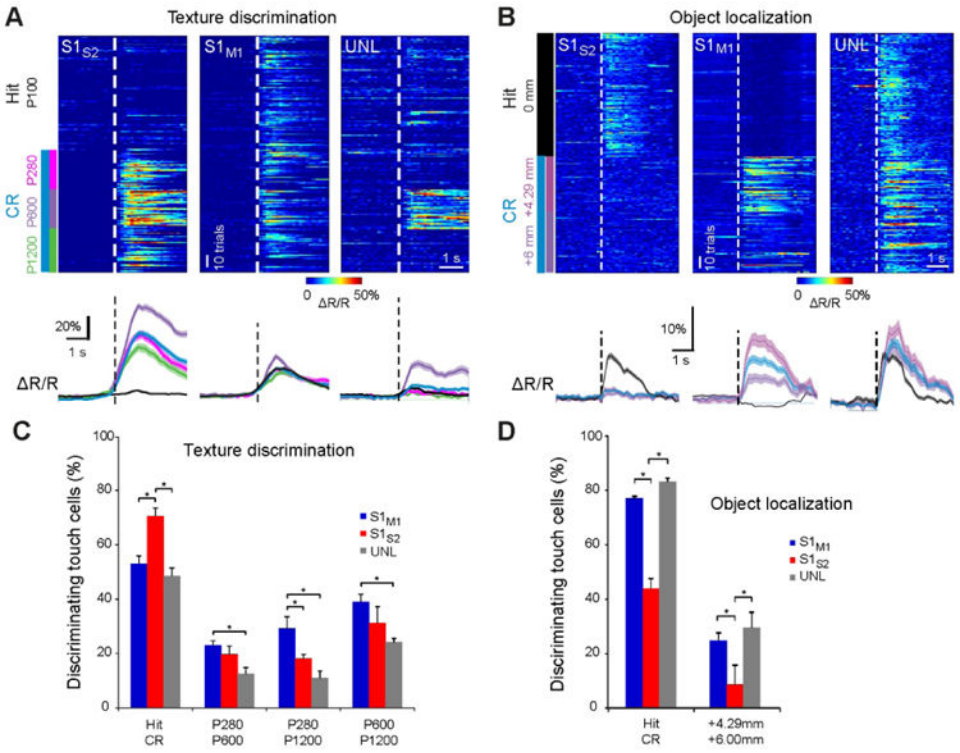

Figure 3.

Single-neuron discrimination analysis of decision or sensory-stimulus features in S1. (A) Top: Single-trial responses of individual $S1_{S2}$, $S1_{M1}$, or UNL example neurons according to Hit/CR trial-type or sandpaper type in the texture discrimination task. Traces are aligned to first touch (dashed line). Color codes for ΔR/R amplitude. All these neurons were classified as touch neurons. Bottom: Average ΔR/R calcium traces of neurons shown on top according to Hit/CR or sandpaper type (shaded regions, s.e.m.). (B) Equivalent plot to (A) but for individual example neurons during the object localization task. (C) Analysis of discrimination power across the touch-neuron population during texture discrimination. Bars indicate the fraction of touch cells discriminating decision or non-target stimuli as determined by ROC analysis across subtypes (* $P < 0.05$, permutation test; error bars, s.d. from permutation test). (D) Equivalent plot to (C) but for touch neurons in the object localization task. All panels adapted from (Chen et al., 2013a).

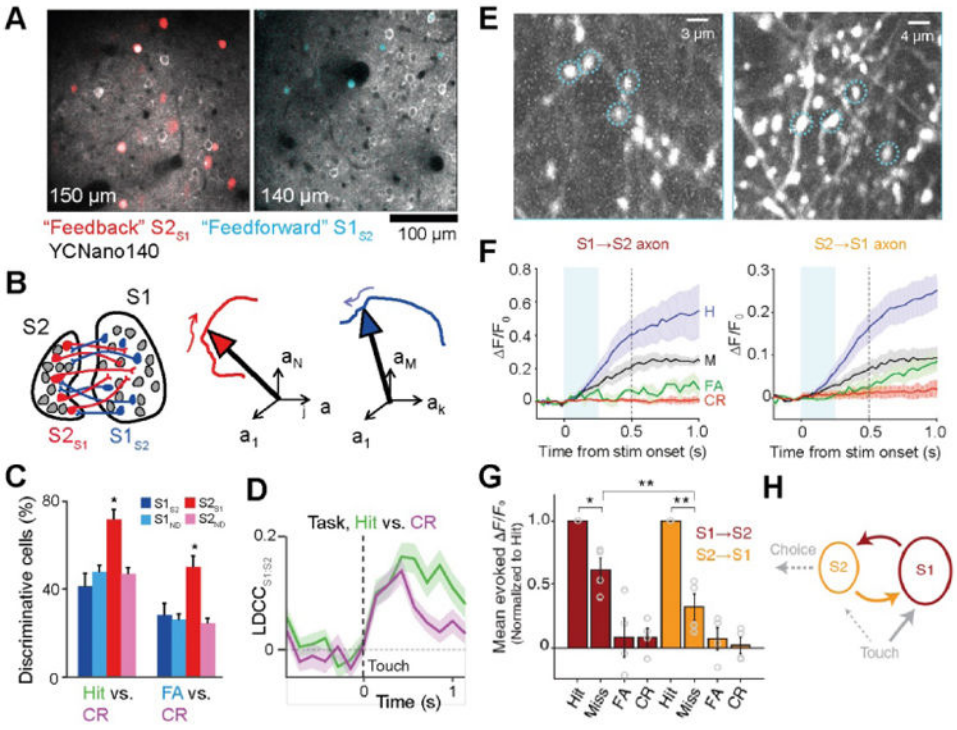

Figure 4.

Neuronal communication between S1 and S2. (A) Simultaneous calcium imaging from S1 and S2 during texture discrimination behavior. In addition to general labeling of excitatory neurons with YCNano140, $S1_{S2}$ neurons (red, left) and $S2_{S1}$ neurons (blue, right) were specifically labeled using retrograde infecting viral vectors. (B) For analysis of neuronal population dynamics the trajectories of state-space vectors were analyzed (using low-dimensional representations by linear discriminant [LD] analysis). (C) Fraction of active neurons discriminating Hit/CR and FA/CR trials above chance determined by single-cell ROC analysis (error bars: s.d. from bootstrap test; $P < 0.05$, χ^2-test; n = 44 $S1_{S2}$, 161 $S1_{ND}$, 59 $S2_{S1}$, 198 $S2_{ND}$ neurons). (D) The correlation of the LD projection of state-space trajectories in S1:S2 (LDCC) increased following touch events and remained high for prolonged time when the animal started licking (Hit trials). (A-D) adapted from (Chen et al., 2016). (E) In mice performing a tactile detection task axon imaging experiments were performed by injecting AAV-GCaMP6 in one region and imaging superficial axons in the target region. Left, example field-of-view showing labeled S1→S2 axons. Right, example field-of-view showing labeled S2→S1 axons. (F) $\Delta F/F_0$ activity (mean ± s.e.m.) of S1→S2 axons (left) and S2→S1 axons (right) for each trial type (averaged across 4 mice each). In both axon types, responses on Hits were larger than on Misses ($P < 0.002$). Cyan shading indicates first 0.25 s after stimulus onset. (G) Mean evoked $\Delta F/F_0$ responses normalized to hits across individual axons (mean ± s.e.m. across mice; circles show individual mice). For both S1→S2 and S2→S1 axons, responses on misses were smaller than on hits. (H) Schematic of feedforward and feedback propagation of task-related activity (dashed: hypothetical functional pathways). (E-H) adapted from (Kwon et al., 2016).

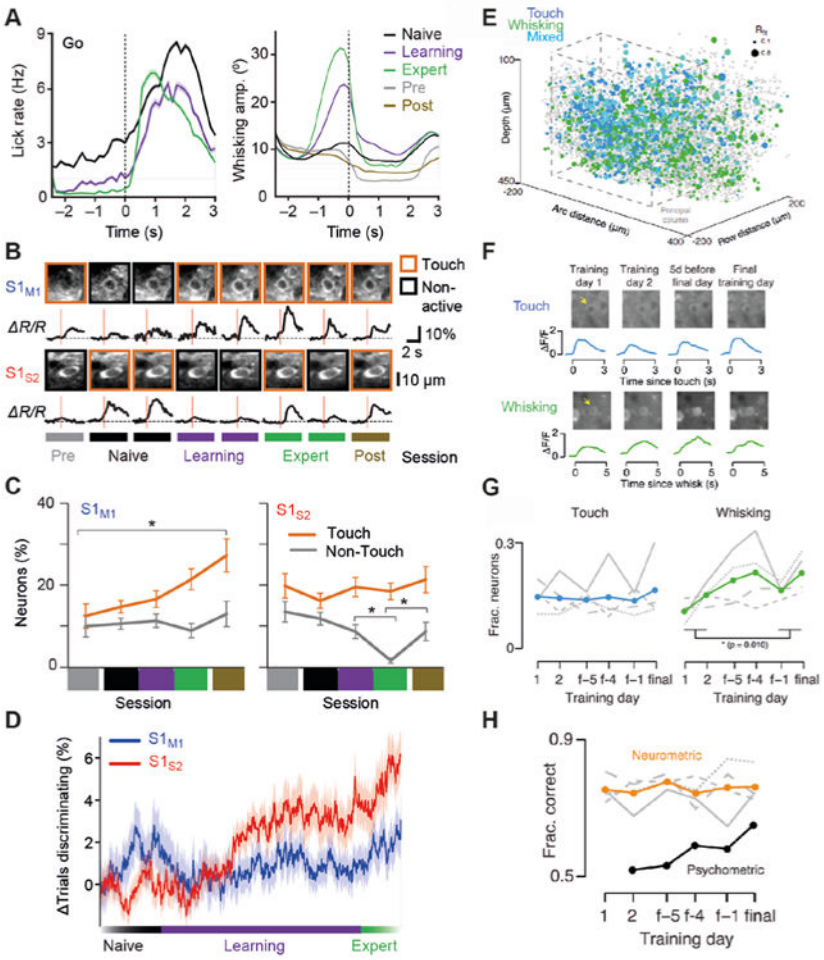

Figure 5.

Functional changes in neocortical dynamics during learning. (A) Time course of lick rate (left) and whisking amplitude (right) aligned to first touch within go trials across different training periods (solid line, mean; shaded area, s.e.m.). In ‘Pre’ and ‘Post’ control sessions textures were presented but without reward or punishment. (B) Longitudinal observation of example $S1_{M1}$ and $S1_{S2}$ neurons across training phases. Across-trial average calcium transients per session, aligned to first touch (red line), are shown. For each session, two-photon images of the neurons are shown on top with the behavior classification per session indicated by the outline box. Neurons were classified as non-active if their calcium responses were not significantly different from the neuropil signal. (C) Distribution of classified neurons across sessions for $S1_{M1}$ and $S1_{S2}$ neurons pooled for all animals. (D) Fraction of trials discriminating relative to naive phase during training across cell types. (A-D) adapted from (Chen et al., 2015). (E) 3D distribution of response types in S1 for the object localization task in one mouse. Blue, touch neurons; green, whisking neurons; cyan, mixed; gray, unclassified; gray dashed line, outline of principal column. Radius indicates R_{fit}. (F) Example neurons imaged during learning of the object localization task (before volume imaging). Left, touch cell; right, whisking cell. (G) Fraction of L2/3 excitatory neurons classified as touch or whisking during learning. Mean touch, blue; mean whisking, green; gray lines, individual animals (n = 4). (H) Neurometric and psychometric

performance over the course of learning. Orange line, task performance of the best ten neuron ensemble; gray lines, individual animals' (n = 4) best ensemble performance; black, cross-animal psychometric performance (the first day of training consisted of a simplified form of the task where the performance metric did not apply and was thus excluded). (E-H) adapted from (Peron et al., 2015).